

Infrared Spectroscopy of Matrix Isolated Polycyclic Aromatic Hydrocarbons. 2. PAHs Containing Five or More Rings

Douglas M. Hudgins* and Scott A. Sandford

National Aeronautics and Space Administration Ames Research Center, MS 245-6,
Moffett Field, California 94035

Received: April 25, 1997[⊗]

Matrix isolation techniques have been used to measure the mid-infrared spectra of the polycyclic aromatic hydrocarbons (PAHs) benzo[*e*]pyrene, pentacene, perylene, benzo[*ghi*]perylene, coronene, and 1,12:2,3:4,5:6,7:8,9:10,11-hexabenzocoronene. The observed band positions and relative strengths are compared to previous lab studies and with theoretical calculations, where available.¹ Agreement with other available laboratory data is excellent. Comparisons with theory indicate that density functional theory (DFT) does an excellent of describing the majority of the infrared active fundamentals of the PAHs considered here. Band positions typically agree to better than 5 cm⁻¹, with the worst disparities usually being less than 15 cm⁻¹. Matches in band strengths are not as precise, but are generally good to better than 30–50% for most strong and moderate bands and are good to factors of 2–4 for weaker bands. The theory predicts CH stretching band strengths that are too strong by a factor of about 2.

I. Introduction

Because of their remarkable stability, polycyclic aromatic hydrocarbons (PAHs) are prevalent in our surroundings and play important roles in the chemistry of fossil fuels, the nucleation and growth of soot particles, as environmental pollutants,^{2–4} and even as interstellar molecules.^{5–7} Despite their importance, reported studies of the vibrational spectroscopic properties of these molecules have, until recently, been limited to PAHs suspended in salt pellets or dispersed in organic solvents.⁸ Since these media are known to strongly perturb the positions and intensities of the fundamental modes of these molecules, we have undertaken a systematic survey of the mid-infrared (4000–500 cm⁻¹) spectra of PAH molecules isolated in argon matrixes. The first results of these studies, on the spectra of small PAHs containing 2–4 benzenoid rings, have been discussed in the preceding article in this journal issue (part 1).⁹ That article also provides a brief review of other current studies of the vibrational spectroscopy of PAHs. This article reports the observed infrared spectroscopic properties of several larger PAHs containing five or more benzenoid rings. The third article of the series, which immediately follows this article in the journal (part 3), addresses the infrared spectral properties of aromatic molecules that incorporate a cyclopentadienyl ring.¹⁰

This paper is organized as follows. Section II presents an overview of the experimental details relevant to these studies. In section III, the spectra of the neutral PAHs are presented and compared to available theoretical and laboratory results, where available. Finally, the findings are summarized in section IV.

II. Experimental Section

The matrix isolation technique was employed to isolate individual polycyclic aromatic hydrocarbon (PAH) molecules in an argon matrix where their infrared spectra were measured.

The experimental apparatus and methodology have been summarized in part 1 and described in detail elsewhere.^{9,11,12}

A PAH vapor stream was generated in a heated Pyrex tube and mixed with argon prior to deposition onto a 10 K CsI window. The PAHs used in this investigation and the temperatures at which they were vaporized were benzo[*e*]pyrene (C₂₀H₁₂), Aldrich 99% purity, $T_{\text{dep}} = 105$ °C; perylene (C₂₀H₁₂), Aldrich, 99+% purity, $T_{\text{dep}} = 120$ °C; benzo[*ghi*]perylene (C₂₂H₁₂), Aldrich, 98% purity, $T_{\text{dep}} = 130$ °C; pentacene (C₂₂H₁₄), Aldrich 98+% purity, $T_{\text{dep}} = 200$ °C; coronene (C₂₄H₁₂), Pfaltz and Bauer 97% purity, $T_{\text{dep}} = 155$ °C; and 1,12:2,3:4,5:6,7:8,9:10,11-hexabenzocoronene (C₄₂H₁₈), 99+% purity (private source), $T_{\text{dep}} = 425$ °C. All samples were used without further purification. Matheson prepurified argon (99.998% min) was used as the matrix material. On the basis of the calibrated argon flow rate and the deposited quantities of pentacene, perylene, benzo[*ghi*]perylene, and coronene calculated from the integrated intensity of the strongest CH out-of-plane bending mode and its theoretical absolute absorption cross section, the argon/PAH ratios in these samples were all well in excess of 1000/1. In addition, assuming an absolute absorption intensity of 110 km/mol for the strongest CH out-of-plane bending modes in benzo[*e*]pyrene and 1,12:2,3:4,5:6,7:8,9:10,11-hexabenzocoronene, a value typical of these bands in other neutral PAHs, it is estimated that the argon/PAH ratios in these samples also exceeded 1000/1. Infrared spectra were measured with a Fourier transform instrument operating at 0.9 cm⁻¹ resolution.

III. Results and Discussion

In the following sections, the infrared spectra and tabular summaries of the measured band positions and relative strengths are presented. First, the aromatic CH stretching spectra (3150–2900 cm⁻¹) of all the PAHs are considered as a group, followed by the individual 2000–500 cm⁻¹ spectra of the PAHs benzo[*e*]pyrene, perylene, benzo[*ghi*]perylene, pentacene, coronene,

* To whom correspondence should be addressed.

[⊗] Abstract published in *Advance ACS Abstracts*, December 15, 1997.

and 1,12:2,3:4,5:6,7:8,9:10,11-hexabenzocoronene, respectively. The strengths and positions of the bands in these spectra are then tabulated and compared to theoretical predictions¹ and other laboratory spectra, where available. The conventions adopted for the presentation of the data are identical with those used in part 1. Briefly, (i) the spectra reflect a small but significant level of H₂O contamination as evidenced by absorption bands in the 1625–1590 cm⁻¹ range. The dominant absorption bands of matrix isolated H₂O fall at 1624, 1608, and 1593 cm⁻¹. Contaminant bands clearly due to H₂O are marked with a solid dot (•) in the spectra. (ii) Multiple bands are tabulated in one of two ways. If one of the bands clearly dominates in strength, only the position of that band is listed with a footnote indicating that it is the strongest member of a band “complex.” In those cases where there is no obvious dominant feature, or where there is reason to believe the bands may be associated with different vibration modes, each individual band position is specified. (iii) Absorption features are tabulated down to an intensity of 1% that of the strongest band in the 900–600 cm⁻¹ aromatic CH out-of-plane bending region. The measured relative band strengths for pentacene, perylene, and coronene are compared with recent density functional theory (DFT) calculations.¹ In those cases where either the experimental or theoretical relative strength of a band exceeds the 1% threshold, but the corresponding to theoretical/experimental value does not, both values are reported. In some cases this necessitated the addition of theoretical bands that did not appear the original publication. Any such bands are noted in the tables. Also, while the theoretical calculations include vibrational modes as low as 90 cm⁻¹, due to detector constraints, the experimental spectra reported here extend only as low as 450 cm⁻¹. (iv) Due to confusion with overtones and combination bands and to the overlapping of fundamental modes, it is difficult to determine the strengths of the aromatic CH stretching features in the 3150–2900 cm⁻¹ region of the experimental spectra. Thus, while the *positions* of all the features in this region are tabulated, only the *total* integrated absorption over the *entire* region is listed. This total absorption is then compared with the *sum* of all the predicted bands in this region, when available.

1. *The CH Stretching Region, 3150–2900 cm⁻¹.* The 3150–2900 cm⁻¹ matrix isolation spectra of all six PAHs can be found in Figures 1a–1f. As mentioned above, comparison between the experimental and theoretical positions and strengths for the CH stretching modes is difficult due to spectral confusion in this region. In general, as was observed and discussed in detail in part 1, the experimental data typically contain more features than predicted by theory, but the strongest features in the experimental data generally fall near the positions of the strongest predicted features. Also consistent with part 1, the theoretical relative intensities are consistently overestimated by a factor of 2. Comparisons with the experimental data for perylene, pentacene, and coronene, the three PAHs for which theoretical calculations are available, yield overestimates of perylene, factor of 1.7; pentacene, 1.8; and coronene, 2.6. These values represent *lower* limits to the mismatches since some of the experimentally measured absorption is due to overtone/combination bands. Most of the theoretical over-estimation is likely due to the relatively small basis set used for the calculations.^{9,13}

2. *Benzo[e]pyrene, C₂₀H₁₂.* The 2000–500 cm⁻¹ spectrum of matrix isolated benzo[e]pyrene is presented in Figure 2. The positions and relative strengths of the absorption bands are listed in Table 1. The relative strengths of the bands were normalized to the strong band pair appearing at 748.2 and 750.0 cm⁻¹.

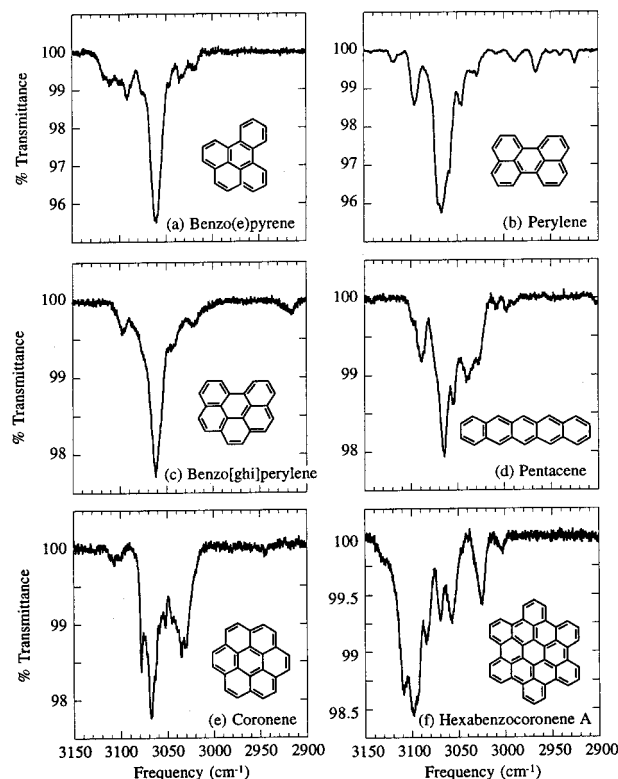


Figure 1. Spectra in the 3150–2900 cm⁻¹ CH stretching region of the matrix isolated PAHs: (a) benzo[e]pyrene (C₂₀H₁₂), (b) perylene (C₂₀H₁₂), (c) benzo[ghi]perylene (C₂₂H₁₂), (d) pentacene (C₂₂H₁₄), (e) coronene (C₂₄H₁₂), and (f) 1,12:2,3:4,5:6,7:8,9:10,11-hexabenzocoronene (hexabenzocoronene A, C₄₂H₁₈). All spectra were taken at a matrix temperature of 10 K. The argon/PAH ratio was in excess of 1000/1 for all the PAHs.

This PAH has not been studied previously either theoretically or using matrix isolation techniques. However, the spectrum of matrix isolated benzo[e]pyrene reported here is in good agreement with its gas-phase spectrum.¹⁴ In the absence of the theoretical calculations it is difficult to assign individual bands to specific vibrational modes. Nevertheless, the general pattern of band positions and strengths is consistent with those of other PAHs (see ref 14 for assignments to general vibrational mode types). The weak bands falling between 1650 and 1950 cm⁻¹ arise from overtone/combination modes rather than fundamental vibrations. The most striking difference between the spectra of benzo[e]pyrene and most other PAHs that have been studied previously is that it contains stronger and more numerous bands in the 1500–1400 cm⁻¹ region than is typical. Although a definitive description of the exact composition of these modes can only be provided by the theory, it is not unreasonable to suggest that this may be due to a selective enhancement in modes involving the asymmetric stretching of the *d* and *f* bonds in the parent pyrene (i.e., in-plane wagging of the pendent benzenoid ring). This species also produces a somewhat atypically large number of bands in the CH out-of-plane bending region, a property shared with 1,2-benzanthracene.⁹ Both molecules contain six nonequivalent classes of CH bonds.

Finally, the band at 1593.2 cm⁻¹ can definitely be assigned to benzo[e]pyrene, although its measured strength may be somewhat uncertain due to contaminant H₂O in the matrix. Also, given this contamination, the presence of other weak benzo[e]pyrene bands in the 1650–1590 cm⁻¹ region cannot be ruled out.

3. *Perylene, C₂₀H₁₂.* The 2000–500 cm⁻¹ spectrum of matrix isolated perylene is presented in Figure 3. The positions

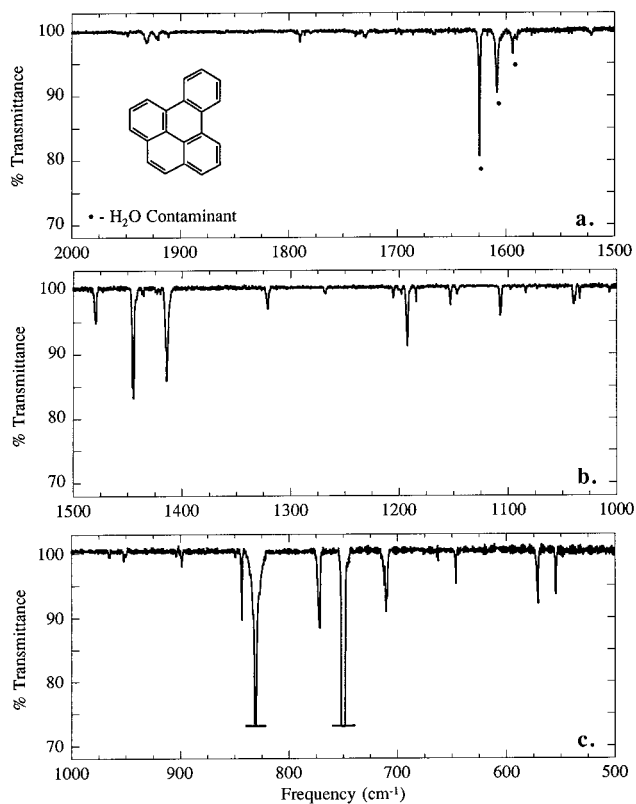


Figure 2. The spectrum of matrix isolated benzo[*e*]pyrene (C₂₀H₁₂) through the aromatic CC stretching and CH bending regions: (a) 2000–1500 cm⁻¹, (b) 1500–1000 cm⁻¹, and (c) 1000–500 cm⁻¹. The spectrum was taken at a matrix temperature of 10 K, and the argon/benzo[*e*]pyrene ratio was estimated to be in excess of 1000/1.

and strengths of the absorption bands are listed and compared to theoretical predictions¹ in Table 2. The relative experimental band strengths were normalized to the strong band at 815.2 cm⁻¹ rather than the stronger 771.6 cm⁻¹ band for reasons that will be discussed below. The theoretical relative band strengths reported for perylene,¹ originally normalized to the predicted 3067.6 cm⁻¹ band, have been renormalized to the predicted 814.5 cm⁻¹ band. Thus, the relative strengths for the theoretical calculations reported in Table 2 have been scaled by a factor of 1.12 relative to those in the original publication (see Table 10 in ref 1).

The agreement in band positions between experiment and theory is excellent. The average difference in the frequencies of predicted and observed bands in Table 2 is only 4 cm⁻¹ and this value would have been considerably smaller if not for a few weak bands that showed large mismatches. Not counting those bands where the assignments may be in doubt, all the frequency differences are less than 15 cm⁻¹. The agreement between relative band strengths is also generally very good, with only the few exceptions discussed below. Strong to moderately strong bands agree to within 30%, while weaker bands agree to better than a factor of 2 to 3.

Several bands listed in Table 2 do require comment. First, there appears to be a large discrepancy between the measured and calculated intensities of the strong 771.6 cm⁻¹ feature. Since this is the strongest absorption feature in the experimental spectrum, it was initially used to normalize the relative band strengths. This, however, resulted in large disparities between experiment and theory for virtually all of the other bands in the perylene spectrum. On the other hand, when the features were normalized to the second strongest band at 815.2 cm⁻¹, agreements for the majority of the bands were vastly improved.

TABLE 1: Infrared Frequencies (cm⁻¹) and Intensities for Neutral Benzo(*e*)pyrene

| frequency in Ar (cm ⁻¹) | relative intensity ^a |
|-------------------------------------|---------------------------------|
| 554.5 | 0.05 |
| 570.6 | 0.07 |
| 645.9 | 0.02 |
| 711.8 ^b | 0.18 |
| 748.2, 750.0 | 1.00 |
| 771.1, 772.1 | 0.15 |
| 830.1 | 0.51 |
| 842.9 | 0.14 |
| 848.8 | 0.01 |
| 898.2 | 0.03 |
| 949.3, 951.5 | 0.02 |
| 964.6 | 0.01 |
| 1006.2 | 0.01 |
| 1037.8, 1039.3 | 0.04 |
| 1083.2 ^b | 0.02 |
| 1106.9 | 0.04 |
| 1152.3 | 0.02 |
| 1183.8 | 0.02 |
| 1191.8 | 0.09 |
| 1204.9 | 0.01 |
| 1267.0, 1268.0 | 0.01 |
| 1320.6 | 0.07 |
| 1413.5 | 0.20 |
| 1434.8, 1436.6 | 0.02 |
| 1444.1, 1444.9 | 0.19 |
| 1478.9 | 0.08 |
| 1593.2 ^c | 0.03 |
| 1665.4 | 0.01 |
| 1728.3 | 0.01 |
| 1789.1 ^b | 0.05 |
| 1919.9, 1922.2 | 0.02 |
| 1930.5 | 0.06 |
| 3018.0 | |
| 3036.0 | |
| 3059.7 ^d | |
| 3091.0 | |
| 3108.7 | |
| Σ 3122–2985 | 1.23 |

^a Intensities relative to that of the combined 748.2 and 750.0 cm⁻¹ bands. ^b Position of strongest band or bands in a “complex” of features. ^c Possibly contains an absorption contribution from contaminant H₂O. ^d Major feature in the CH stretching region.

This suggests that the calculated strength of the 771.6 cm⁻¹ feature is underestimated by about a factor of 3 (theory, 0.53; experiment, 1.45). This is very surprising since the agreement between the experiment and theory for the stronger bands in other PAH spectra has always been better than 50%.

While not as dramatic, several other band comparisons require comment. The observed band at 1500.1 cm⁻¹ is about a factor of 2 larger than predicted (theory, 0.06; experiment, 0.11), while the observed band at 1573.1 cm⁻¹ is about 4 times weaker (theory, 0.08; experiment, 0.02), although the latter discrepancy may be an artifact of H₂O contamination. Finally, an absorption band is observed near 1613.9 cm⁻¹ that corresponds to the predicted feature at 1596.4 cm⁻¹, but its intensity cannot be determined to any degree of accuracy due to obscuration by contaminant H₂O.

These findings are in overall good agreement with previous matrix isolation studies of perylene¹⁶ (see also Table 10 in ref 1). While the work presented here significantly extends the sensitivity of the spectral measurements, for the most part, where comparisons are possible, measured positions routinely match to within the stated accuracy (1 cm⁻¹). The weak band observed at 1494.2 cm⁻¹ in these earlier experiments, is not, however, detected here, but if the previous data were normalized to the 815.2 cm⁻¹ band (rather than the 771.6 cm⁻¹ band), the intensity

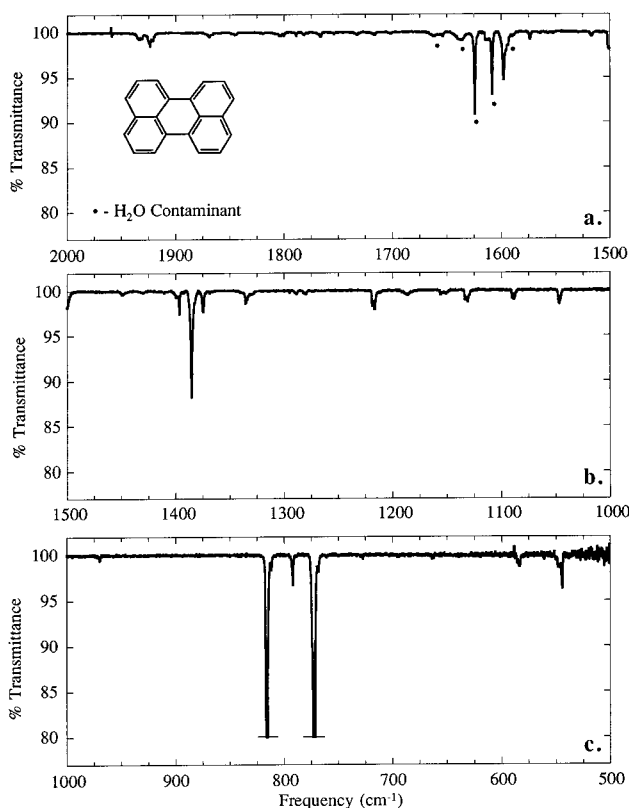


Figure 3. The spectrum of matrix isolated perylene ($C_{20}H_{12}$) through the aromatic CC stretching and CH bending regions: (a) 2000–1500 cm^{-1} , (b) 1500–1000 cm^{-1} , and (c) 1000–500 cm^{-1} . The spectrum was taken at a matrix temperature of 10 K, and the argon/peryene ratio was in excess of 1000/1.

of that band would fall near the 0.01 threshold of the data reported here. Both data sets agree that the 771.6 cm^{-1} band is substantially stronger than the 815.2 cm^{-1} rather than the other way around as predicted by the theory. Both data sets also agree on the larger than average position mismatch for the 1335.2 cm^{-1} band and the weakness of the feature predicted to have moderate strength near 1573 cm^{-1} . Indeed, no band is even reported at this position in the earlier work. The largest difference between the data sets involves the 1335.2, 1385.1, and 1500.1 cm^{-1} bands, all of which are around twice as strong as reported in the earlier matrix isolation studies. As a result, the value reported here falls closer to the predicted strength of the 1335.2 cm^{-1} band, the previously reported value falls closer to the prediction for the 1500.1 cm^{-1} band, and the two data sets straddle the strength prediction for the 1385.1 cm^{-1} band.

4. *Benzo[ghi]perylene*, $C_{22}H_{12}$. The 2000–500 cm^{-1} spectrum of matrix isolated benzo[ghi]perylene is presented in Figure 4. The positions and strengths of the absorption bands are listed in Table 3. The relative strengths of the bands were normalized to the strong band at 846.3 cm^{-1} .

The infrared spectrum of this PAH has not been previously studied either theoretically or using matrix isolation techniques. However, the observed matrix isolation spectrum reported here is in good agreement with the data from gas-phase benzo[ghi]perylene.¹⁴ In the absence of the theoretical calculations it is difficult to assign individual bands to specific vibrational modes. However, the general pattern of band positions and strengths show many of the characteristics typical of other PAHs (see ref 14 for assignments to general vibrational mode types). Both benzo[ghi]perylene, together with benzo[e]pyrene above, are C_{2v} molecules and, thus, of lower symmetry than the other PAHs

TABLE 2: Infrared Frequencies (cm^{-1}) and Intensities for Neutral Perylene

| experiment | | theory ^a | | | |
|-------------------------------|---------------------------------|----------------------------|-------------------------|--------------------|---------------------------------|
| frequency in Ar (cm^{-1}) | relative intensity ^b | irreducible representation | frequency (cm^{-1}) | intensity (km/mol) | relative intensity ^c |
| <i>d</i> | | b_{3u} | 175.9 | 4.7 | 0.04 |
| <i>d</i> | | b_{1u} | 462.0 | 2.5 | 0.02 |
| 544.1 | 0.10 | b_{3u} | 545.2 | 8.1 | 0.07 |
| 583.1 | 0.05 | b_{1u} | 579.4 | 3.0 | 0.02 |
| 771.6 | 1.45 | b_{3u} | 765.3 | 63.0 | 0.53 |
| | | b_{2u} | 774.5 | 2.7 | 0.02 |
| 791.4 | 0.06 | b_{1u} | 792.7 | 7.7 | 0.07 |
| 811.2 | 0.02 | b_{1u} | 807.0 | 4.2 | 0.03 |
| 815.2 | 1.00 | b_{3u} | 814.5 | 119.8 | 1.00 |
| 969.5 | 0.02 | b_{3u} | 981.7 | 2.6 | 0.02 |
| 1046.7 | 0.05 | b_{2u} | 1042.8 | 3.1 | 0.02 |
| 1088.1, 1089.8 | 0.04 | b_{1u} | 1091.4 | 2.5 | 0.02 |
| 1130.6, 1133.2 | 0.06 | b_{2u} | 1134.7 | 4.1 | 0.03 |
| 1150.4, 1155.7 | 0.03 | b_{1u} | 1156.7 [†] | 1.06 | 0.02 |
| 1185.8 | 0.04 | b_{2u} | 1200.4 [†] | 1.1 | 0.02 |
| 1216.2, 1218.5 | 0.09 | b_{1u} | 1216.9 | 5.9 | 0.04 |
| 1279.4 | 0.01 | b_{2u} | 1272.1 | 2.8 | 0.02 |
| 1288.2 | 0.02 | | | | |
| 1294.5 | 0.01 | | | | |
| 1335.2 | 0.09 | b_{2u} | 1329.4 | 8.7 | 0.08 |
| | | b_{1u} | 1349.4 | 3.0 | 0.02 |
| 1374.3 | 0.07 | | | | |
| 1385.1 | 0.44 | b_{1u} | 1387.0 | 36.0 | 0.30 |
| 1396.2, 1399.2 | 0.07 | | | | |
| 1430.0 | 0.01 | | | | |
| 1448.8 | 0.02 | b_{1u} | 1446.8 | 3.9 | 0.03 |
| 1467 | <i>vw</i> | b_{2u} | 1469.1 [†] | 1.7 | 0.01 |
| 1500.1 | 0.11 | b_{2u} | 1495.3 | 6.2 | 0.06 |
| 1516.5 | 0.02 | | | | |
| 1573.1 | 0.02 | b_{1u} | 1572.8 | 9.6 | 0.08 |
| 1597.5 ^e | 0.25 | b_{1u} | 1586.0 | 23.8 | 0.20 |
| 1613.9 ^e | 0.04 | b_{2u} | 1596.4 | 9.5 | 0.08 |
| 1653.3 ^e | 0.02 | | | | |
| 1715.5 | 0.02 | | | | |
| 1732.1 | 0.02 | | | | |
| 1765.7 | 0.02 | | | | |
| 1777.9, 1781.0 | 0.02 | | | | |
| 1803.0 ^f | 0.04 | | | | |
| 1844.8 | 0.02 | | | | |
| 1868.6 | 0.03 | | | | |
| 1920.4, 1923.0 | 0.08 | | | | |
| 1930.9, 1933.0 | 0.04 | | | | |
| 2948.9 | | | | | |
| 3007 | | | | | |
| 3022 | | | | | |
| 3046 | | b_{2u} | 3048.7 | 7.8 | 0.07 |
| 3065.9 ^g | | b_{1u} | 3067.6 | 134.5 | 1.12 |
| 3095.0 | | b_{2u} | 3068.5 | 34.7 | 0.29 |
| 3117.7 | | b_{1u} | 3084.8 | 8.9 | 0.07 |
| | | b_{2u} | 3099.3 | 68.8 | 0.57 |
| Σ 3125–2940 | 1.24 | | | | |
| sum = | | | | 254.7 | 2.124 |

^a Taken from ref 1. [†] indicates band not reported in original publication. ^b Intensities relative to the strongest band at 815.2 cm^{-1} . ^c Theoretical intensities relative to the strength of the calculated 814.5 cm^{-1} band. Relative values are a factor of 1.12 larger than those reported in ref 1. ^d Theoretical position lying below the low-frequency limit of experimental data. ^e Strength uncertain because of potential contributions from contaminant H_2O . ^f Position of strongest band in a “complex” of features. ^g Major feature in the CH stretching region.

considered in this paper, which explains the relative richness of their spectra.

The only band that warrants specific comment is the band at 1602.1 cm^{-1} , which arises from benzo[ghi]perylene but whose measured strength may contain some contribution from contaminant H_2O . Other benzo[ghi]perylene bands may also be present in the 1650–1590 cm^{-1} region, but obscuration by H_2O bands prevents their detection.

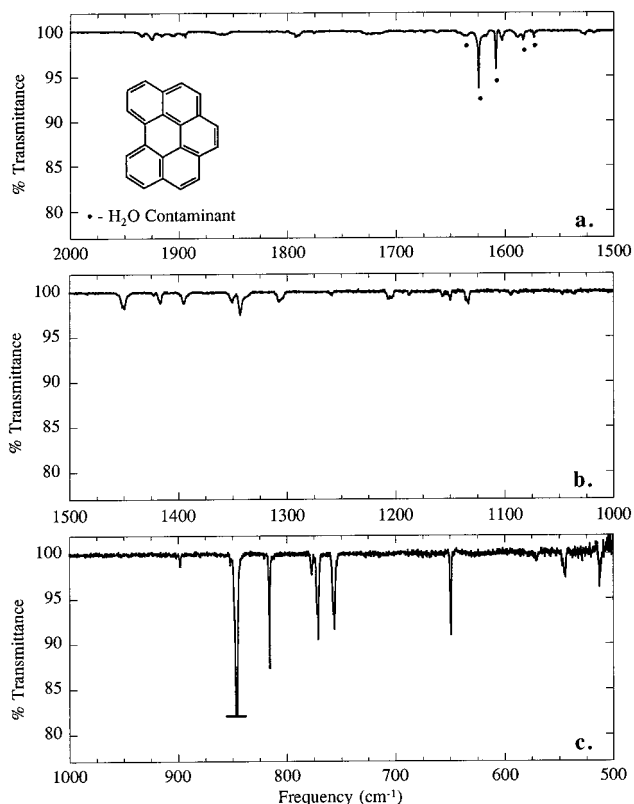


Figure 4. The spectrum of matrix isolated benzo[*ghi*]perylene ($C_{22}H_{12}$) through the aromatic CC stretching and CH bending regions: (a) 2000–1500 cm^{-1} , (b) 1500–1000 cm^{-1} , and (c) 1000–500 cm^{-1} . The spectrum was taken at a matrix temperature of 10 K, and the argon/benzo[*ghi*]perylene ratio was in excess of 1000/1.

5. *Pentacene*, $C_{22}H_{14}$. The 2000–500 cm^{-1} spectrum of matrix isolated pentacene is presented in Figure 5. The positions and strengths of the absorption bands are listed in Table 4 together with their theoretically predicted values.¹ The relative strengths of the experimental bands were normalized to the band at 899.9 cm^{-1} . The theoretically predicted band strengths, originally normalized to the 3078.5 cm^{-1} band in ref 1, have renormalized here to the predicted 914.5 cm^{-1} band. Thus, the relative strengths that are reported for the theory in Table 4 have been scaled by a factor of 1.39 relative to the values appearing in the original publication (see Table 5 in ref 1).

The agreement in band positions between experiment and theory is generally very good. The average difference in the frequencies of predicted and observed bands in Table 4 is around 8 cm^{-1} , and not counting a few extremely weak bands where the assignments may be in doubt, all the frequency differences are less than 15 cm^{-1} . While this match is very good, it is not as good as that observed for most of the other PAHs examined. The amount of mismatch is not significantly decreased if only the strongest bands are considered, suggesting that the difference is not simply due to the misidentification of some of the weaker bands.

A comparison of relative band strengths shows a similar pattern—the agreement between experiment and theory is satisfactory, but not as good as that observed for other PAHs. In two to four ring PAHs, the intensities of most strong and moderate bands (except in the CH stretching region) were found to agree to better than 35% and weaker bands to within factors of 2–3.⁹ In the case of pentacene, the relative strengths of the stronger bands agree to within about 60% with the *average* mismatch being about 35%. Moderately strong bands are generally fit somewhat better, although one band disagrees by

TABLE 3: Infrared Frequencies (cm^{-1}) and Intensities for Neutral Benzo[*ghi*]perylene

| frequency in Ar (cm^{-1}) | relative intensity ^a |
|-------------------------------|---------------------------------|
| 512.5 | 0.07 |
| 544.2 | 0.09 |
| 570.0 | 0.02 |
| 648.9 | 0.14 |
| 755.8, 756.9 | 0.30 |
| 770.9 | 0.25 |
| 776.8 | 0.05 |
| 815.5 | 0.18 |
| 846.3 | 1.00 |
| 851.8 | 0.01 |
| 897.9 | 0.02 |
| 968.3 | 0.01 |
| 1036.3 | 0.02 |
| 1087.8 | 0.01 |
| 1093.4 | 0.01 |
| 1132.7 ^b | 0.06 |
| 1149.2 | 0.03 |
| 1155.4, 1156.9 | 0.01 |
| 1186.9 | 0.01 |
| 1206.7 ^b | 0.07 |
| 1259.1 ^b | 0.01 |
| 1302.9, 1307.0 | 0.07 |
| 1342.6 | 0.22 |
| 1350.0 | 0.05 |
| 1394.7 | 0.08 |
| 1416.0, 1417.1 | 0.06 |
| 1422.1 | 0.01 |
| 1449.0, 1451.1 | 0.13 |
| 1517.8 | 0.01 |
| 1527.4 | 0.02 |
| 1602.1 ^c | 0.04 |
| 1673.3 | 0.01 |
| 1726 | 0.11 |
| 1792.1 ^b | 0.02 |
| 1859.6 | 0.06 |
| 1893.4 | 0.02 |
| 1903.5, 1905.7 | 0.02 |
| 1915.6 | 0.02 |
| 1923.4, 1925.9 | 0.04 |
| 1932.0, 1933.8 | 0.01 |
| 2916 | |
| 3019.8 | |
| 3041.2 | |
| 3060.8 ^d | |
| 3096.4 | |
| Σ 3109–2902 | 1.35 |

^a Intensities relative to the strongest band at 846.3 cm^{-1} . ^b Position of strongest band or bands in a “complex” of features. ^c Strength uncertain because of potential contributions from contaminant H_2O . ^d Major feature in the CH stretching region.

more than a factor of 2 (see below). Weaker bands all agree to within better than factors of 2 to 3.

Several of the other bands listed in Table 2 require some additional comment. First, theory predicts fairly weak bands at 1132.5 and 1174.2 cm^{-1} (relative intensities 0.03 and 0.002, respectively) that are hard to reconcile with the experimental spectrum. A pair of bands is observed at 1164.1 and 1165.3 cm^{-1} which have a strength (0.02) appropriate to the 1132.5 cm^{-1} band, but which would imply a remarkably large frequency difference (>30 cm^{-1}). Conversely, while the predicted 1174.2 cm^{-1} band provides a much more satisfying agreement in position, this would imply a dramatic difference between the measured and calculated relative intensities. The experimental bands at 1334.5 cm^{-1} (0.02) and 1350.5 cm^{-1} (0.07) are similarly difficult to assign. If the observed 1350.5 cm^{-1} band corresponds to the predicted band at 1351.9 cm^{-1} (0.01), then its intensity is 7 times stronger than that predicted and the weak

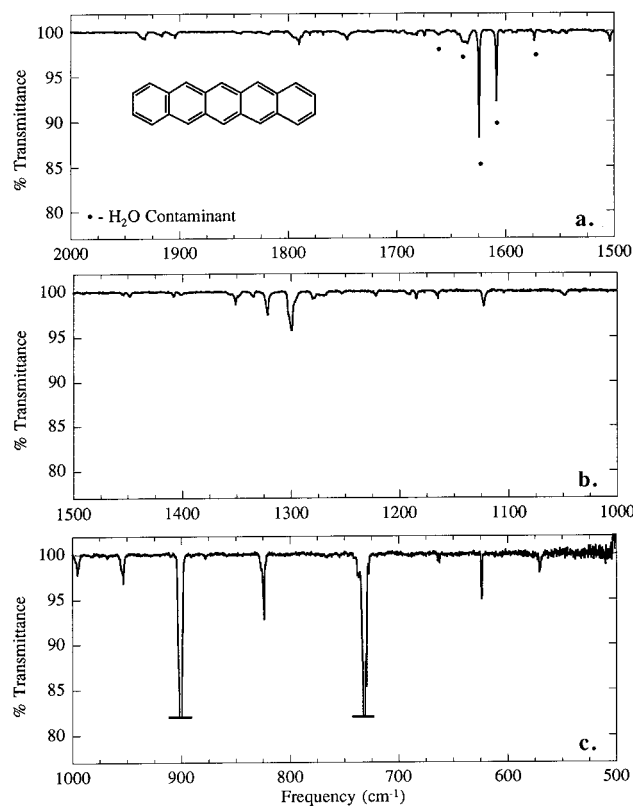


Figure 5. The spectrum of matrix isolated pentacene ($C_{22}H_{14}$) through the aromatic CC stretching and CH bending regions: (a) 2000–1500 cm^{-1} , (b) 1500–1000 cm^{-1} , and (c) 1000–500 cm^{-1} . The spectrum was taken at a matrix temperature of 10 K, and the argon/pentacene ratio was in excess of 1000/1.

band at 1334.5 cm^{-1} is unexplained. On the other hand, if the observed 1334.5 cm^{-1} band corresponds to the predicted 1351.9 cm^{-1} band, then the strength match is better, but the difference between the experimental and theoretical frequencies is atypically large, and it leaves the band at 1350.5 cm^{-1} unexplained.

Finally, there also may be a strength mismatch for the moderately strong feature predicted at 1623.1 cm^{-1} and seen at 1634.2/1639.0 cm^{-1} . The observed absorption is approximately a factor of 2 less than expected (theory, 0.11; experiment, 0.06). However, the observed band falls very close to an H_2O contaminant band, making the measured strength uncertain.

These findings are in overall good agreement with previous matrix isolation studies of pentacene¹⁵ (see also Table 5 in ref 1). Where comparisons are possible, the measured positions routinely match to within experimental accuracy with only a few exceptions. There are a few bands that appear in Table 4 that were not reported previously,¹⁵ but most of these have relative strengths of 0.03 or less and presumably simply fell below the strength threshold of the earlier experiments. The good agreement between the two data sets further verifies the main discrepancies between the experimental measurements and the theoretical calculations. The previous studies also show no evidence for the predicted 1132.5 cm^{-1} band but do report an absorption band at 1164.3 cm^{-1} . Also, both the 1350.5 and 1334.5 cm^{-1} bands, one of which has no theoretical counterpart, were reported in the previous matrix study. The measured strength reported for the 1634.2 cm^{-1} feature is also substantially less than the theory would indicate.

Interestingly, of the smaller PAHs discussed in part 1, the greatest discrepancies were encountered with tetracene which is the next smaller member of the polyacene family. Thus, it may be that the theory has increasing difficulty with the

TABLE 4: Infrared Frequencies (cm^{-1}) and Intensities for Neutral Pentacene

| experiment | | theory ^a | | | |
|-------------------------------|---------------------------------|----------------------------|-------------------------|--------------------|---------------------------------|
| frequency in Ar (cm^{-1}) | relative intensity ^b | irreducible representation | frequency (cm^{-1}) | intensity (km/mol) | relative intensity ^c |
| <i>d</i> | | b_{3u} | 461.8 | 21.8 | 0.21 |
| <i>d</i> | | b_{3u} | 468.7 | 5.1 | 0.06 |
| <i>d</i> | | b_{2u} | 482.8 | 7.3 | 0.07 |
| 570.2 | 0.03 | b_{1u} | 572.5 | 2.6 | 0.03 |
| 623.4 | 0.05 | b_{2u} | 634.1 | 4.9 | 0.04 |
| 727.0 | 0.01 | b_{2u} | 724.7 | 4.7 | 0.04 |
| 731.3 ^e | 0.82 | b_{3u} | 735.4 | 73.4 | 0.71 |
| 823.7 | 0.15 | b_{3u} | 829.2 | 19.4 | 0.19 |
| 877.4 | 0.01 | b_{2u} | 862.8 [†] | 0.1 | 0.001 |
| 890.3 | <i>vw</i> | b_{1u} | 911.5 | 2.0 | 0.01 |
| 899.9 | 1.00 | b_{3u} | 914.5 | 102.4 | 1.00 |
| 952.8 ^e | 0.07 | b_{3u} | 961.7 | 10.7 | 0.10 |
| 995.1 | 0.06 | b_{2u} | 991.8 | 3.7 | 0.04 |
| 1047.7 | 0.02 | | | | |
| 1122.1 | 0.05 | b_{1u} | 1117.7 | 5.5 | 0.06 |
| | | b_{2u} | 1132.5 | 2.9 | 0.03 |
| 1164.1, 1165.3 | 0.02 | b_{2u} | 1174.2 [†] | 0.2 | 0.002 |
| 1184.0 | 0.02 | b_{1u} | 1198.0 | 2.4 | 0.03 |
| 1191.0 | 0.01 | | | | |
| 1221.1 | 0.01 | b_{2u} | 1228.6 [†] | 1.3 | 0.02 |
| 1269 | 0.02 | | | | |
| 1278.7 | 0.02 | b_{1u} | 1283.3 [†] | 1.0 | 0.01 |
| 1298.9 | 0.24 | b_{1u} | 1290.8 | 24.1 | 0.24 |
| 1320.9 | 0.08 | b_{2u} | 1331.8 | 11.5 | 0.11 |
| 1334.5 | 0.02 | | | | |
| 1350.5 | 0.07 | b_{1u} | 1351.9 [†] | 1.0 | 0.01 |
| 1400.2 | 0.04 | b_{2u} | 1395.1 [†] | 1.0 | 0.01 |
| 1407.2 | 0.02 | | | | |
| 1447.8 | 0.01 | b_{1u} | 1444.6 [†] | 0.9 | 0.01 |
| 1453.9 | 0.01 | b_{2u} | 1449.0 [†] | 1.2 | 0.01 |
| 1503.3 | 0.04 | b_{2u} | 1503.1 | 2.4 | 0.03 |
| 1543.3 | 0.01 | b_{2u} | 1530.7 [†] | 1.6 | 0.02 |
| 1573.0 | 0.02 | | | | |
| 1600.7 | 0.01 | b_{1u} | 1593.8 [†] | 0.6 | 0.01 |
| 1634.2, 1639.0 ^f | 0.06 | b_{1u} | 1623.1 | 11.6 | 0.11 |
| 1673.7 | 0.01 | | | | |
| 1745.1 ^e | 0.04 | | | | |
| 1789.2 ^e | 0.10 | | | | |
| 1903.5 ^e | 0.03 | | | | |
| 1915.4 ^e | 0.02 | | | | |
| 1931.1 ^e | 0.06 | | | | |
| 2997 | | | | | |
| 3007 | | | | | |
| 3026.5 | | | | | |
| 3039.6 | | b_{1u} | 3038.9 | 2.6 | 0.03 |
| | | b_{2u} | 3042.5 | 5.2 | 0.06 |
| | | b_{1u} | 3043.1 | 9.4 | 0.10 |
| | | b_{1u} | 3044.9 | 53.2 | 0.51 |
| | | b_{2u} | 3048.5 | 5.3 | 0.06 |
| 3053.7 | | b_{1u} | 3063.9 | 81.5 | 0.79 |
| 3063.7 ^g | | b_{2u} | 3078.5 | 142.8 | 1.39 |
| 3088.1 | | | | | |
| 3096.9 | | | | | |
| Σ 3107–2987 | 1.67 | | | | |
| sum = | | | | 300.0 | 2.93 |

^a Taken from ref 1. [†] indicates band not reported in original publication. ^b Intensities relative to the strongest band at 899.9 cm^{-1} . ^c Theoretical intensities relative to the strength of the calculated 914.5 cm^{-1} band. Relative values are a factor of 1.39 larger than those in original publication. ^d Theoretical position lying below the low-frequency limit of experimental data. ^e Position of strongest band in a “complex” of features. ^f Possibly contains an absorption contribution from contaminant H_2O . ^g Major feature in the CH stretching region.

polyacene structure with increasing size. Conversely, it could be that matrix perturbations become increasingly important as the length of the polyacene chain grows.

6. *Coronene*, $C_{24}H_{12}$. The 2000–500 cm^{-1} spectrum of matrix isolated coronene is presented in Figure 6. Experimental and theoretical positions and strengths of the absorption bands are listed in Table 5. The relative strengths of the measured

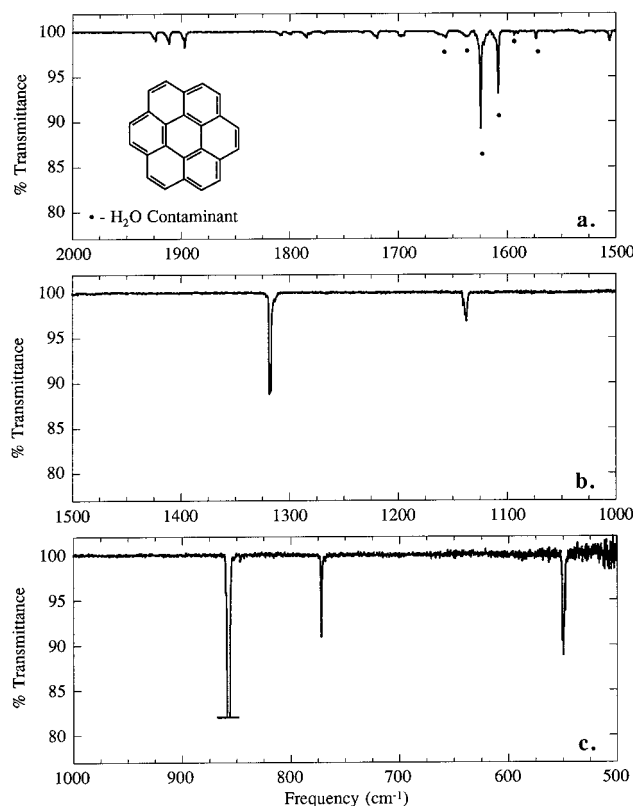


Figure 6. The spectrum of matrix isolated coronene ($C_{24}H_{12}$) through the aromatic CC stretching and CH bending regions: (a) 2000–1500 cm^{-1} , (b) 1500–1000 cm^{-1} , and (c) 1000–500 cm^{-1} . The spectrum was taken at a matrix temperature of 10 K, and the argon/coronene ratio was in excess of 1000/1.

experimental bands were normalized to the 857.0 cm^{-1} band and those of the theory, originally normalized to the theoretical 3064.9 cm^{-1} CH stretching band in ref 1, were renormalized initially to the predicted 864.4 cm^{-1} band. However, when this was done, the relative intensities of the theoretical bands were consistently lower than observed, implying some uncertainty in the strength of the theoretical 864.4 cm^{-1} . When, instead, the theoretical bands were scaled to match the relative strength of the theoretical 549.0 cm^{-1} band to that of the experimental 550.5 cm^{-1} band (0.27), a much more satisfactory overall agreement between the data sets is obtained. Thus, the theoretical relative strengths for coronene reported in Table 5 have been scaled by a factor of about 2.69 relative to those in the original publication (see Table 12 in ref 1).

Because of its high degree of symmetry (D_{6h}), coronene produces a relatively simple spectrum for such a large molecule. The agreement between experiment and theory is generally very good. Where band correspondences are clear, the average difference in the frequencies of predicted and observed bands is 5 cm^{-1} and all the frequency differences are less than about 12 cm^{-1} . Relative band strengths also compare favorably, although there are a few notable exceptions. As mentioned above, one of the largest discrepancies involves the 857.0 cm^{-1} experimental band, the strongest band in the spectrum, which has a measured intensity 40% less than predicted (theory, 1.69; experiment, 1.00). Furthermore, there is a substantial discrepancy for the moderately strong predicted band at 1602.7 cm^{-1} . Although H_2O contaminates this region, such a strong band (theory, 0.24) near this frequency should be clearly evident. An experimental band is observed at about 1620.7 cm^{-1} that probably corresponds to this feature, but while its strength can

TABLE 5: Infrared Frequencies (cm^{-1}) and Intensities for Neutral Coronene

| experiment | | theory ^a | | | |
|-------------------------------|---------------------------------|----------------------------|-------------------------|--------------------|---------------------------------|
| frequency in Ar (cm^{-1}) | relative intensity ^b | irreducible representation | frequency (cm^{-1}) | intensity (km/mol) | relative intensity ^c |
| <i>d</i> | | b_{3u} | 123.9 | 4.9 | 0.05 |
| <i>d</i> | | e_u | 378.5 | 6.3 | 0.05 |
| 550.5 ^e | 0.27 | b_{3u} | 549.0 | 27.9 | 0.27 |
| 771.6 | 0.11 | e_u | 774.6 | 11.7 | 0.11 |
| 846.1 | 0.01 | | | | |
| 857.0 | 1.00 | b_{3u} | 864.4 | 175.8 | 1.69 |
| 1137.0 ^e | 0.11 | e_u | 1140.3 | 13.0 | 0.13 |
| 1210.7, 1214.6 | vw | e_u | 1214.4 [†] | 2.0 | 0.02 |
| 1317.4, 1318.3 | 0.32 | e_u | 1312.4 | 48.1 | 0.46 |
| 1497.9 | 0.01 | | | | |
| 1505.3 | 0.03 | e_u | 1494.8 | 2.7 | 0.03 |
| 1530.4, 1533.0 | 0.02 | | | | |
| 1579.2 | 0.01 | | | | |
| 1620.7 ^f | 0.04–0.08 | e_u | 1602.7 | 26.3 | 0.24 |
| 1695.5 | 0.04 | | | | |
| 1718.7 | 0.04 | | | | |
| 1767.6 | 0.01 | | | | |
| 1783.8 | 0.03 | | | | |
| 1798.7 | 0.01 | | | | |
| 1808.0 | 0.02 | | | | |
| 1896.0 | 0.05 | | | | |
| 1910.4 | 0.05 | | | | |
| 1922.9, 1924.4 | 0.04 | | | | |
| 2943.0 | | | | | |
| 3029.2 ^g | | | | | |
| 3034.3 ^g | | | | | |
| 3044.4 | | e_u | 3042.8 | 15.6 | 0.16 |
| 3051.4 | | e_u | 3064.9 | 279.8 | 2.69 |
| 3066.8 ^g | | | | | |
| 3077.2 ^g | | | | | |
| 3099.0 | | | | | |
| 3105.9 | | | | | |
| 3110.3 | | | | | |
| Σ 3089–2938 | 1.09 | | | | |
| sum = | | | | 295.4 | 2.85 |

^a Taken from ref 1. [†] indicates band not reported in original publication. ^b Intensities relative to the strongest band at 857.0 cm^{-1} . ^c Theoretical intensities scaled so the calculated 549.0 cm^{-1} band has the same strength as the experimentally observed band at 550.5 cm^{-1} (0.27). Relative values are a factor of 2.69 larger than those in original publication. ^d Theoretical position lying below the low-frequency limit of experimental data. ^e Position of strongest band in a “complex” of features. ^f Possibly contains an absorption contribution from contaminant H_2O . ^g Major features in the CH stretching region.

only be estimated (0.04–0.08), it appears to be significantly weaker than predicted.

Finally, these results are in excellent agreement with previous matrix isolation studies of coronene^{17,18} (see also Table 12 ref 1). While a number of the weaker features reported here have not been reported previously, where comparisons are possible, measured positions routinely match to within 1–2 cm^{-1} . Presumably, the additional features reported here simply fell below the detection threshold in the earlier experiments. Notably, those data sets confirm the overestimates in the intensities of the 864.4 and 1602.7 cm^{-1} theoretical bands.

7. *1,12:2,3:4,5:6,7:8,9:10,11-hexabenzocoronene, C₄₂H₁₈*. The 2000–500 cm^{-1} spectrum of matrix isolated 1,12:2,3:4,5:6,7:8,9:10,11-hexabenzocoronene (hereafter hexabenzocoronene A) is presented in Figure 7. The positions and strengths of the absorption bands are listed in Table 6. The relative strengths of the bands were normalized to the strong band at 772.4 cm^{-1} . A spectrum of solid-state hexabenzocoronene A evaporated onto KBr has been published by Wdowiak.¹⁹ While no band positions, intensities, or assignments were tabulated by Wdowiak, qualitative comparison of the spectra indicates that the two spectra are at least consistent with each other.

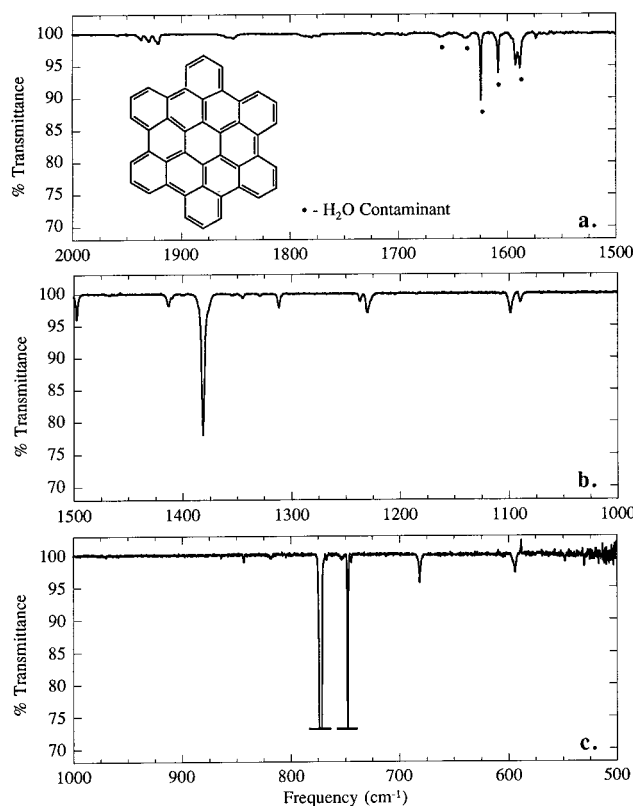


Figure 7. The spectrum of matrix isolated 1,12:2,3:4,5:6,7:8,9:10,11-hexabenzocoronene (hexabenzocoronene A, $C_{42}H_{18}$) through the aromatic CC stretching and CH bending regions: (a) 2000–1500 cm^{-1} , (b) 1500–1000 cm^{-1} , and (c) 1000–500 cm^{-1} . The spectrum was taken at a matrix temperature of 10 K, and the argon/hexabenzocoronene A ratio was in excess of 1000/1.

Cyvin and Cyvin²⁰ have used a simple five-parameter force-field approximation for condensed aromatics to calculate the in-plane and out-of-plane vibrational frequencies of hexabenzocoronene A. However, as this model did not calculate expected band strengths, it is very difficult to assign the calculated frequencies to specific bands in the matrix isolation spectrum. Correspondences that leave a minimum of unmatched bands generally lead to average frequency mismatches on the order of 40–50 cm^{-1} . This suggests that theoretical calculations of the spectra of larger PAHs will require more sophisticated calculations such as those presented here and in the previous paper⁹ for smaller PAHs. Unfortunately, at this time, such calculations require a prohibitive amount of computation time.

In the absence of the theoretical calculations that provide fairly precise band positions and strengths it is difficult to assign individual bands to specific vibrational modes. Again, the general pattern of band positions and strengths show many of the characteristics typical of other PAHs and the types of vibrational modes associated with the various spectral regions are expected to be the same. As was the case for coronene, despite its size, the high degree of symmetry of this molecule (D_{6h}) results in a relatively simple spectrum.

As with all the other PAHs examined by matrix isolation techniques, the presence of small amounts of contaminant H_2O complicates the detection of absorption bands in the 1650–1580 cm^{-1} region. Thus, while no bands are reported in this region, such bands may be present but obscured by the features of contaminant H_2O .

TABLE 6: Infrared Frequencies (cm^{-1}) and Intensities for Neutral Hexabenzocoronene A

| frequency in Ar (cm^{-1}) | relative intensity ^a |
|-------------------------------|---------------------------------|
| 530.2 | 0.01 |
| 548.0 | 0.01 |
| 593.7 | 0.05 |
| 681.1 | 0.06 |
| 744.2 | 0.01 |
| 747.4 ^b | 0.24 |
| 772.4 ^b | 1.00 |
| 818.1 | 0.01 |
| 842.8 | 0.01 |
| 1089.3 | 0.03 |
| 1098.3 | 0.08 |
| 1229.4 | 0.08 |
| 1236.4 | 0.02 |
| 1311.1 | 0.04 |
| 1344.3 | 0.01 |
| 1380.8 | 0.66 |
| 1409.2, 1412.6 | 0.06 |
| 1497.0 | 0.07 |
| 1562.8, 1567.7 | 0.01 |
| 1587, 1591.7 ^c | 0.17 |
| 1779.0 ^b | 0.05 |
| 1851.5, 1857.2 | 0.03 |
| 1920.6 | 0.04 |
| 1929.1 | 0.03 |
| 1936.2 | 0.02 |
| 3002.2 | |
| 3024.6 | |
| 3056.5 | |
| 3068.6 | |
| 3083.4 | |
| 3097.8 ^d | |
| 3108.0 ^d | |
| 3131 | |
| Σ 3141–2996 | 0.74 |

^a Intensities relative to the strongest visible band at 772.4 cm^{-1} .

^b Position of strongest band or bands in a “complex” of features.

^c Contains an absorption contribution from contaminant H_2O . ^d Major features in the CH stretching region.

IV. Conclusions

The 4000–500 cm^{-1} infrared absorption spectra of six different PAHs that contain five or more aromatic rings have been measured. The samples were prepared using standard argon matrix isolation techniques. The resulting band positions and relative strengths were compared to previous lab studies and with theoretical calculations, where available. Where comparisons can be made, there is excellent agreement with previous matrix isolation studies and good agreement with gas-phase studies.

Comparisons with the theoretical calculations for the PAHs pentacene, perylene, coronene, and hexabenzocoronene A demonstrate that density functional theory (DFT) is generally accurate to within 5 cm^{-1} in predicting the positions of the infrared active fundamentals PAHs while simple force-field calculations exhibit substantially larger uncertainties on the order of 50 cm^{-1} . The worst discrepancies between experiment and DFT theoretical predictions usually involve weak bands where the band assignments may be in question and where matrix effects are correspondingly more important, and even in these cases the discrepancies are rarely more than 15 cm^{-1} .

Agreement in band strengths are not as precise as matches in frequencies, but are generally good to better than 30–50% for most strong and moderate bands and are good to factors of 2–4 for weaker bands. The larger difference for the weak bands may be partially due to the increased importance of matrix effects. Despite the generally good match between experiment

and theory, individual PAH spectra can contain a small number of moderate or strong bands that show significant differences between experiment and theory. These strength mismatches rarely exceed a factor of 2.

As with the smaller PAHs, the most consistent difference between the experimental and theoretical results lies in the CH stretching region. Theory consistently predicts band intensities that are too strong by about a factor of 2. This mismatch in intensities is supported by other available matrix isolation and gas-phase studies of PAHs.

Comparisons between the infrared spectra of matrix isolated neutral PAHs and the interstellar emission band family characteristic of UV-rich environments indicate that neutral PAHs do not provide an overall good fit to the vast majority of the astronomical data. Readers interested in a more detailed discussion of the astrophysical importance of neutral PAHs are directed to the discussion and references included in part 1.⁹

Acknowledgment. The authors thank S. Langhoff and C. Bauschlicher for providing unabridged versions of their computational results, L. Allamandola for advice and support during this research, R. Walker for expert technical assistance, and T. Wdowiak for providing a sample of 1,12:2,3:4,5:6,7:8,9:10,11-hexabenzocoronene. Mass spectral analysis of this sample was provided by S. Clemmett and S. Gillett at Stanford University, and their support is also appreciated. This work was carried out under NASA Grants 344-02-06-01 (Astrophysics Program) and 459-60-61-01 (Long Term Space Astrophysics Program).

References and Notes

- (1) Langhoff, S. R. *J. Phys. Chem.* **1996**, *100*, 2819.
- (2) (a) Lee, M. L.; Novotny, M. V.; Bartle, K. D. *Analytical Chemistry of Polycyclic Aromatic Compounds*; Academic Press: New York, 1981; Chapter 2. (b) Yürüm, Y., Ed. *New Trends in Coal Science*; NATO ASI Series, Series C: Mathematical and Physical Sciences; Kluwer Academic Publishers: Dordrecht, 1988; Vol. 244.
- (3) (a) Harris, S. J.; Weiner, A. M. *Combust. Sci. Technol.* **1983**, *31*, 155. (b) Frenklach, M.; Warnatz, J. *Combust. Sci. Technol.* **1987**, *51*, 265.
- (4) Harvey, R. G., Ed. *Polycyclic Hydrocarbons and Carcinogenesis*; American Chemical Society: Washington, DC, 1985.
- (5) (a) Duley, W. W.; Williams, D. A. *Mon. Not. R. Astron. Soc.* **1981**, *196*, 269. (b) Leger, A.; Puget, J. L. *Astron. Astrophys.* **1984**, *137*, L5. (c) Allamandola, L. J.; Tielens, A. G. G. M.; Barker, J. R. *Astrophys. J.* **1985**, *290*, L25.
- (6) Allamandola, L. J.; Tielens, A. G. G. M.; Barker, J. R. *Astrophys. J., Suppl. Ser.* **1989**, *71*, 733.
- (7) Witteborn, F. C.; Sandford, S. A.; Bregman, J. D.; Allamandola, L. J.; Cohen, M.; Wooden, D. *Astrophys. J.* **1989**, *341*, 270.
- (8) For examples, see: (a) Lippencott, E. R.; O'Reilly, E. J. *J. Chem. Phys.* **1955**, *23*, 238 and references therein. (b) Cyvin, S. J.; Cyvin, B. N.; Brunvoll, J.; Whitmer, J. C.; Klaeboe, P.; Gustavsen, J. E. *Z. Naturforsch.* **1979**, *34A*, 876. (c) Cyvin, B. N.; Klaeboe, P.; Whitmer, J. C.; Cyvin, S. J. *Z. Naturforsch.* **1982**, *37A*, 251. (d) Cyvin, S. J.; Cyvin, B. N.; Brunvoll, J.; Whitmer, J. C.; Klaeboe, P. *Z. Naturforsch.* **1982**, *37A*, 1359.
- (9) Hudgins, D. M.; Sandford, S. A. *J. Phys. Chem. A* **1997**, *329*.
- (10) Hudgins, D. M.; Sandford, S. A. *J. Phys. Chem. A* **1997**, *356*.
- (11) Bauschlicher, C. W., Jr.; Langhoff, S. R.; Sandford, S. A.; Hudgins, D. M. *J. Phys. Chem. A*, **1997**, *101*, 2414.
- (12) (a) Hudgins, D. M.; Sandford, S. A.; Allamandola, L. J. *J. Phys. Chem.* **1994**, *98*, 4243. (b) Hudgins, D. M.; Allamandola, L. J. *J. Phys. Chem.* **1995**, *99*, 3033. (c) Hudgins, D. M.; Allamandola, L. J. *J. Phys. Chem.* **1995**, *99*, 8978.
- (13) Bauschlicher, C. W., Jr.; Langhoff, S. R. *Spectrochim. Acta A*, **1997**, *53*, 1225.
- (14) Semmler, J.; Yang, P. W.; Crawford, G. E. *Vib. Spectrosc.* **1991**, *2*, 189.
- (15) Szczepanski, J.; Wehlburg, C.; Vala, M. *Chem. Phys. Lett.* **1995**, *232*, 221.
- (16) Szczepanski, J.; Chappo, C.; Vala, M. *Chem. Phys. Lett.* **1993**, *205*, 434.
- (17) Szczepanski, J.; Vala, M. *Astrophys. J.* **1993**, *414*, 646.
- (18) Joblin, C.; d'Hendecourt, L.; Léger, A.; Defourneau, D. *Astron. Astrophys.* **1994**, *281*, 923.
- (19) Wdowiak, T. J. *Solid State Astrophysics*. In Proceedings of the International School of Physics "Enrico Fermi" Course CXI; Bussoletti, E., Strazzula, G., Eds.; North-Holland: Amsterdam, 1991; p 279.
- (20) Cyvin, B. N.; Cyvin, S. J. *Spectrosc. Lett.* **1986**, *19*, 1161.